Original article
https://doi.org/10.18019/1028-4427-2026-32-2-244-253

Features of adjacent joint structures remodeling after prosthetic application of a tibial calcium-phosphate coated implant

T.A. Stupina[1]✉, A.A. Emanov[1], V.P. Kuznetsov[1,2]

[1] Ilizarov National Medical Research Centre for Traumatology and Orthopedics, Kurgan, Russian Federation
[2] Ural Federal University named after the First President of Russia B.N. Yeltsin, Ekaterinburg, Russian Federation

Corresponding author: Tatyana A. Stupina, StupinaSTA@mail.ru

Abstract

Introduction Studying the reorganization of adjacent joint components due to prosthesis application and identifying predictors of arthrosis are key factors to successful functional restoration of a prosthetic limb.

The **aim** of this study was to evaluate the structural reorganization of the basic joint components after prosthetic application of a calcium phosphate-coated implant at long term.

Materials and Methods The study was conducted on five intact and six experimental mongrel male dogs, aged 1.8 ± 0.5 years and weighing 19.0 ± 1.2 kg. A tibial stump was modeled at the level of the upper third of the diaphysis. A Ti6Al4V calcium-phosphate coated implant was used 2.5 months later. The study was conducted at six and 12 months after prosthesis application. Histomorphometry of the synovial membrane and osteochondral component of the tibial plateau was performed on semithin and paraffin sections using an AxioScope.A1 microscope with Zenblue software (CarlZeissMicroImagingGmbH, Germany).

Results Mild synovitis detected at six months (hyperplasia of the integumentary layer, predominance of macrophage-like synoviocytes, plasma cells, and mast cells) was reversible in 70 % of cases at 12 months. Signs of impaired synovial blood supply were recorded. Articular cartilage changes according to the OARSI scale corresponded to grades 0–1 at six months and grades 1–2 at 12 months (in one case, synovial pannus). Basophilic line abnormalities were noted: vessel density (number of vessels per unit of visual field analyzed) was (0.35 ± 0.02) at six months and (0.30 ± 0.02) at 12 months. Differences between time points were statistically insignificant, $p = 0.736$. Subchondral bone plate thickness was significantly ($p = 0.0105$) lower than in the control. At 12 months, the median subchondral bone plate thickness was 33 % higher than the one in the control animals, and the bone index was 31 % higher; differences were statistically significant. Active osteoblasts that were lining bone trabeculae were noted at all stages; fuchsinophilic structures predominated in the bone matrix when stained with Masson's method.

Discussion The histological signs of inflammation and impaired blood supply to the synovial membrane, thinning of the articular cartilage, and invasion of the synovial pannus into the superficial zone and vessels into the deep cartilage zone were prognostic markers of osteoarthritis.

Conclusion Structural changes in the osteochondral component of the tibial plateau one year after application of a tibial calcium phosphate-coated implant were consistent with the initial stage of osteoarthritis. Mild non-infectious synovitis was reversible. The use of calcium phosphate-coated implants promoted the activation of reparative osteogenesis and mineralization of the bone matrix in the subchondral zone.

Keywords: exoprosthetics, calcium phosphate-coated implant, synovial membrane, osteochondral component, morphometry

For citation: Stupina TA, Emanov AA, Kuznetsov VP. Features of adjacent joint structures remodeling after prosthetic application of a tibial calcium-phosphate coated implant. *Genij Ortopedii*. 2026;32(2):244-253. doi: 10.18019/1028-4427-2026-32-2-244-253.

INTRODUCTION

Osteointegrative exoprosthetics of limbs is an advanced technology for the restoration of lost limbs by integrating a metal implant with the bone tissue of the stump, thus providing a stable and functional connection [1, 2, 3, 4]. The advantages of this method include improved functionality and quality of life of patients, sensory feedback (osteoperception and osteoproprioception), long-term function and elimination of problems associated with traditional socket prostheses (skin irritation, poor fit, high incidence of bone and/or soft tissue pain, allergic reactions, decreased function and further deterioration in quality of life) [5, 6, 7, 8, 9].

Current research on improving the osteointegrative properties of implants is aimed at increasing the efficiency of bone tissue bonding with the implant by modifying its surface (microtexturing, nanostructured and biologically active coatings), stimulating osteogenesis (electrical stimulation, use of drugs that stimulate mineralization) [10, 11, 12, 13].

It was established that calcium-phosphate coated implants have high biocompatibility and accelerate the process of osseointegration [14, 15].

Animal studies showed that in the adjacent joint, six months after tibial prosthesis application with a PressFit implant, structural changes in the articular cartilage corresponded to grade 0–1 according to the Osteoarthritis Association for the Study of Osteoarthritis (OARSI) classification [16]. Structural changes in the subchondral zone corresponded to stage 0 according to the classification of Aho et al. [17] what indicates “very early signs of osteoarthritis” [18]. When calcium phosphate-coated implants were installed in the overlying joint, the processes of subchondral bone resorption and articular cartilage thinning were expressed to a lesser extent compared to uncoated implants [19].

In patients with limb amputation, a common complication after prosthetic fiting is contractures and arthrosis in the adjacent joint, which arise due to factors such as increased stress on the joint, impaired biomechanics, prolonged joint immobility, muscle weakness, and the body's inflammatory response to implants [20, 21].

Disorders in the normal joint biomechanics and the presence of infection foci which may develop after prosthesis application [5] are among the main causes of synovitis development.

Studying the features of the structural reorganization of the components of the joint adjacent to the prosthesis and identifying predictors of arthrosis are the key to successful restoration of the function of the prosthetic limb and long-term service life of the prosthesis.

The **aim** of this study was to evaluate the structural reorganization of the basic joint components after prosthetic application of a calcium phosphate-coated implant at long term.

MATERIAL AND METHODS

Study design

The study was performed on 11 mongrel dogs (males) aged (1.8 ± 0.5) years, with a body weight of (19.0 ± 1.2) kg. A tibial stump at the level of the upper third of the diaphysis was modeled in experimental animals (n = 6). After 2.5 months, a calcium-phosphate coated implant made of Ti6Al4V alloy was applied (Patent for Utility Model of the Russian Federation No. 194912, [23]). Next, using the Ilizarov apparatus and a special device (Patent of the Russian Federation No. 185647, [24]), the implant was fixed and compression was applied to the bone (F_{load} = 20 N) for 35 days after the surgery, after which an exoprosthesis was fitted. The time-points of the follow-ups were six and 12 months after prosthesis application.

Study objects were synovial membrane, articular cartilage and subchondral bone of the tibial plateau.

As a control group, the synovial membrane, articular cartilage and subchondral zone of the tibial plateau of five intact dogs were examined.

Ethical statement

The study was conducted in accordance with the European Convention (ETS No. 123) for the Protection of Vertebrate Animals used for Experimental and other Scientific Purposes and state standards (GOST 33044-2014). The study was approved by the institutional ethics board (protocol dated November 29, 2024, No. 1(76)).

Euthanasia

Euthanasia was performed after muscle relaxation with a solution of 1 % diphenhydramine (0.02 mg/kg) and 2 % rometar (5 mg/kg) by administering a lethal dose of barbiturates.

Histological methods of study

For histomorphometric analysis, the knee joint was opened, fragments of the synovial membrane were excised, and articular cartilage samples with underlying subchondral bone were excised from weight-bearing areas of the tibial plateau. The excised osteochondral blocks were fixed in 10 % neutral formalin and then decalcified in a mixture of formic and hydrochloric acids (a standard gentle decalcification protocol was used, which does not significantly affect the tinctorial properties of the bone matrix). Subsequent paraffin embedding of the osteochondral blocks was performed in a HISTOSAFE™ INFILTRA™ vacuum tissue embedding apparatus (ErgoProduction LLC, Russia). Sections 5–7 μm thick from paraffin blocks were prepared on a Thermo Scientific HM 450 microtome (USA), stained with hematoxylin and eosin; to identify the degree of mineralization of the bone matrix, a special three-color staining method according to Masson was used [25].

To analyze angiogenesis, an immunohistochemical study was performed to determine the presence of the CD34 marker (rabbit monoclonal antibodies to CD34 [EP373Y]) (Abcam, UK). To visualize the reaction, a reagent kit for the immunohistochemical detection of HRP/DAB (ab236469 — Rabbit-specific HRP/DAB Detection IHC Detection Kit-Micropolymer, Abcam, UK) was used. All stages of the reaction were carried out according to the protocol of the antibody manufacturer. Sections were counterstained with hematoxylin.

Synovial membrane samples were dehydrated after aldehyde-osmium fixation and embedded in a two-component epoxy resin. Semithin (0.5–1.0 μm) sections (4–8 mm^2) were prepared on a Nova ultramicrotome (LKB, Sweden) and stained with methylene blue and basic fuchsin.

The study at the light-optical level was carried out using an AxioScope.A1 microscope with an AxioCam digital camera (CarlZeissMicroImagingGmbH, Germany).

Histomorphometry using Zenblue software (CarlZeissMicroImagingGmbH, Germany) was used to determine the following parameters in the articular cartilage: thickness of uncalcified cartilage ($h_{uncal.cr}$, μm) and thickness of calcified cartilage ($h_{cal.cr}$, μm). In the deep zone of uncalcified cartilage, the vessel occurrence was assessed (the ratio of the sum of vessels in the visual fields to the number of all analyzed visual fields). An average of 20 fields was analyzed in each animal at a magnification of 400×. In the subchondral zone, the thickness (height) of subchondral bone plate (h_{CtTh}, μm) was determined, and the bone index was calculated as the ratio of the thickness of trabeculae (TbTh, μm) to the width of the intertrabecular spaces (ItTh, μm).

The severity of structural changes in the articular cartilage was assessed according to the OARSI histological classification [16], structural changes in the subchondral zone were assessed according to the classification of Aho et al. [17], and the severity of the inflammatory process in the synovial membrane was assessed according to the scale of Krenn et al. [26].

Statistical methods

Quantitative data were processed in a Microsoft Excel spreadsheet. The Kolmogorov test was used to assess the sample distribution type. The measure of central tendency of the parameters is

presented as the median and quartiles, minimum and maximum values (Me ($p25$–$p75$) [min–max]), and as the mean and standard error of the mean (M ± m). The Mann – Whitney test was used to analyze differences between the compared groups, and the Barnard test was used for frequency indicators; differences were considered significant at $p < 0.05$ (AtteStat software, version 9.3.1).

RESULTS

Structural reorganization of the synovial membrane

After six months of the experiment, synovial cells in the synovial membrane in the inner layer were arranged in one to three layers, with macrophage-like synoviocytes predominating. Those cells had an ovoid nucleus, cytoplasmic outgrowths, and basophilic cytoplasm containing numerous granules and vacuoles (Fig. 1a). Collagen fibers predominated in the superficial collagen-elastic layer, the cellularity was moderately increased, and plasma cells and mast cell clusters were recorded along with fibrocytes and fibroblasts (Fig. 1b). Vessels with thickened walls due to smooth muscle cell hypertrophy were seen in the deep collagen-elastic layer; in some vessels, swollen endothelial cell nuclei blocked the intravascular space (Fig. 1c).

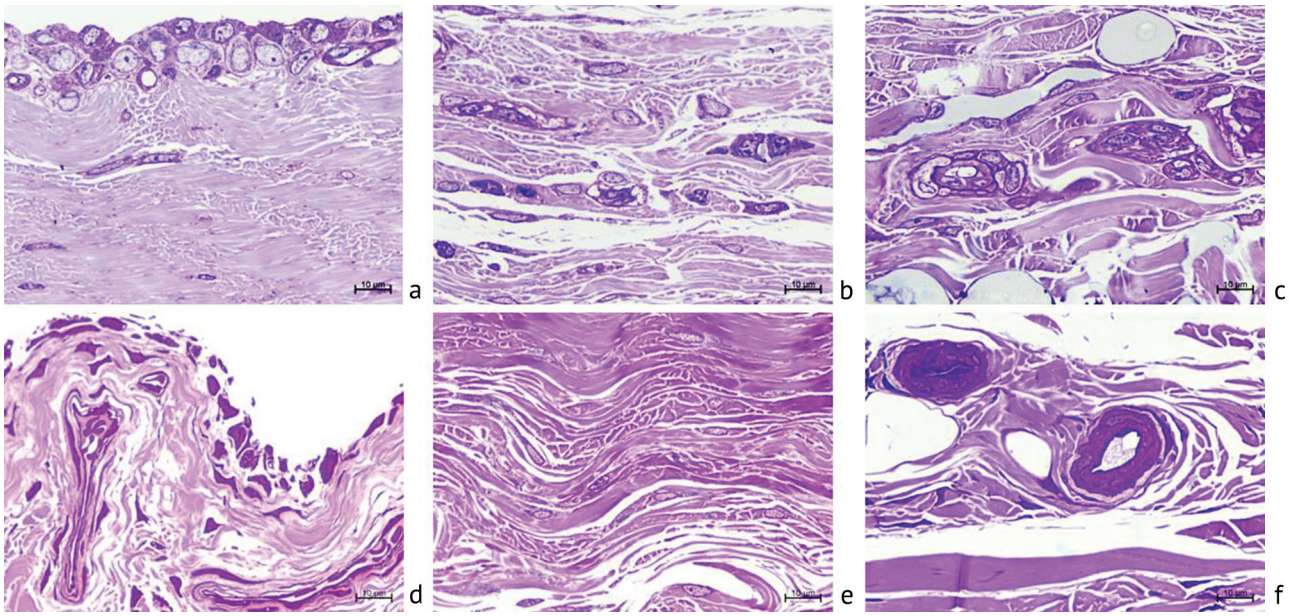

Fig. 1 Synovial membrane of the knee joint at the experiment time points: (a, b, c) six months; (d, e, f) 12 months. Macrophage-like synoviocytes (a) and destructively altered synoviocytes (d) predominate in the inner layer. In the upper collagen-elastic layer there are fibroblasts, fibrocytes, mast and plasma cells (b), fibrocytes (e). Changes in vessels in the deep collagen-elastic layer (c, f). Semi-thin sections; stained with methylene blue and basic fuchsin; magnification ×1000

After 12 months of the experiment, areas of thickening of the inner layer were noted, in which synovial cells were arranged in three to four layers, the majority of synoviocytes showing signs of destruction, an abnormal shape, and pyknotic nuclei (Fig. 1d). In the superficial collagen-elastic layer, normal cellularity and singly located fibroblasts and fibrocytes were preserved (Fig. 1e), and an increase in optical voids between the fibers was noted. In the deep collagen-elastic layer, vessels had thickened walls and stenosis (Fig. 1f).

Structural reorganization of articular cartilage

The articular cartilage of the tibial condyles in the experiment, as in the control group, retained its zonal structure, with all cartilage zones clearly defined. In the superficial zone, after six months of the experiment, most observations showed a decrease in the proportion of the cellular component and an increase in the proportion of acellular areas, along with a disruption of the homogeneity

of the intercellular substance (Fig. 2b). After 12 months of the experiment, one of three observations showed synovial pannus invasion into the superficial zone of the cartilage, with empty cellular lacunae (Fig. 2c).

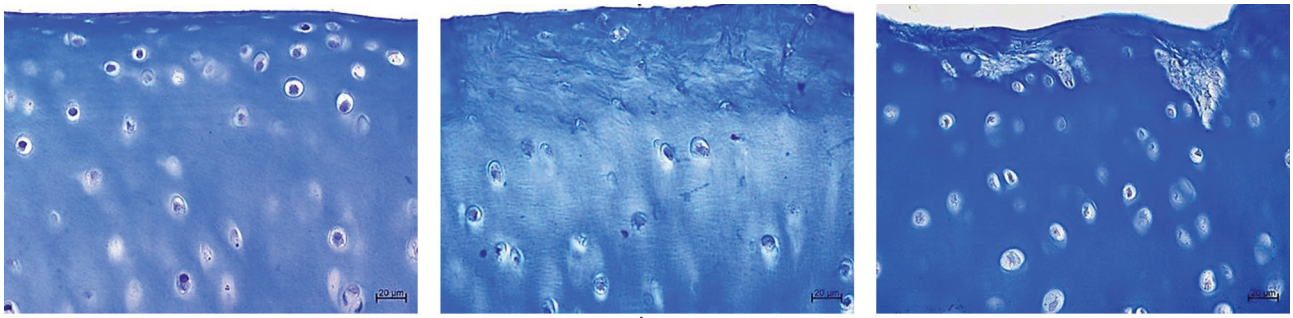

Fig. 2 Superficial and part of the intermediate zone of the lateral condyle of the tibia: (a) control (intact norm); (b) six months of the experiment, unmasking of collagen fibers, acellular fields in the superficial and intermediate zones; (c) 12 months of the experiment, ingrowth of the synovial pannus. Paraffin sections, stained with the three-color method according to Masson. Magnification ×400

Throughout the experiment, cytoarchitecture was preserved in the intermediate and deep zones, with cell-free fields and some cells exhibiting signs of chondroptosis. Areas of discontinuity of the basophilic line and vascular and bone marrow pannus invasion into the deep zone of non-calcified cartilage were recorded (Fig. 3). The frequency of vessel occurrence in the deep zone after six months of the experiment was (0.35 ± 0.02) and (0.30 ± 0.02) after 12 months; the differences were statistically insignificant (p = 0.736).

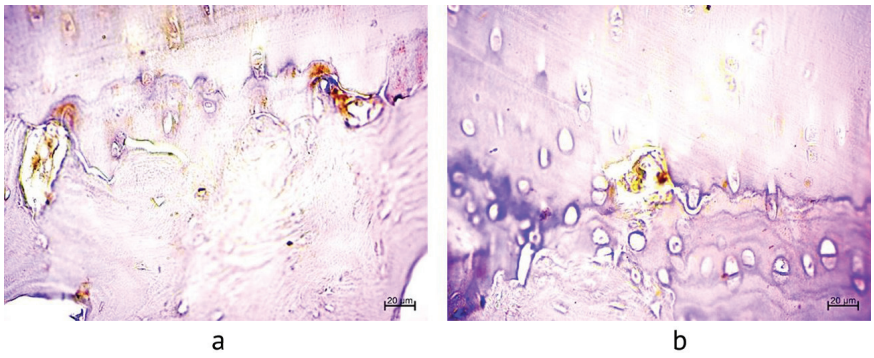

Fig. 3 CD34 expression in vessel endothelium (brown sediment). Disruption of basophilic line continuity, vascular invasion into the deep zone of cartilage: (a) six months of the experiment; (b) 12 months of the experiment. Paraffin sections. Magnification ×400

Structural reorganization of the subchondral zone

In intact animals (control group), the subchondral bone plate was of uneven thickness and continuous; fuchsinophilic structures predominated in the bone matrix when stained with the Masson three-color method (Fig. 4a). In the experimental series, the thickness of the subchondral bone plate varied; thinning areas were more common at six months of the experiment, while thickened areas were more common at 12 months. Staining with the Masson three-color method showed a decrease in the proportion of fuchsinophilic structures after six months (Fig. 4b), and after 12 months the proportion of fuchsinophilic structures increased again (Fig. 4c), indirectly indicating increased bone matrix mineralization.

Throughout the experiment, areas of the subchondral bone plate lined with active osteoblasts producing the main substance were recorded (Fig. 4 b, c).

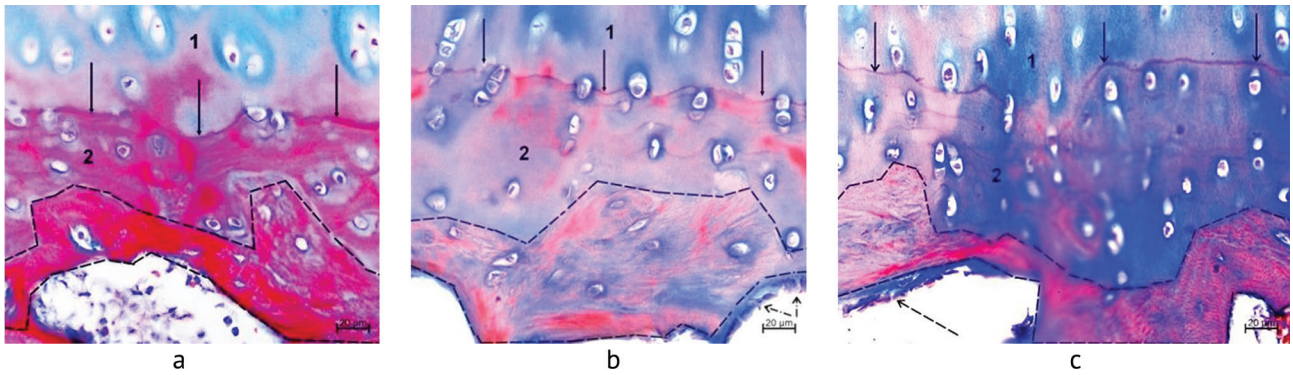

Fig. 4 Contact of calcified cartilage with the subchondral bone plate: (a) control; (b) six months of the experiment; (c) 12 months of the experiment. Designations: 1 — deep zone of non-calcified cartilage; 2 — calcified cartilage; dotted line — borders of the subchondral bone plate; solid arrows — basophilic line; dotted arrows — osteoblasts. Paraffin sections. Staining by the three-color method according to Masson. Magnification ×400

At all stages of the experiment, signs of reparative osteogenesis were observed in the subchondral trabecular bone: active osteoblasts lining the surfaces of bone trabeculae (Fig. 5). The bone trabecular network was sparse, and the trabecular surfaces were partially lined with osteoblasts (Fig. 5a). Staining with the Masson three-color method revealed that the bone trabecular matrix was predominantly red (Fig. 5b). The bone trabeculae and subchondral bone plate were thickened (Fig. 5c). Osteoblasts were present on the surface of the bone trabeculae (Fig. 5d).

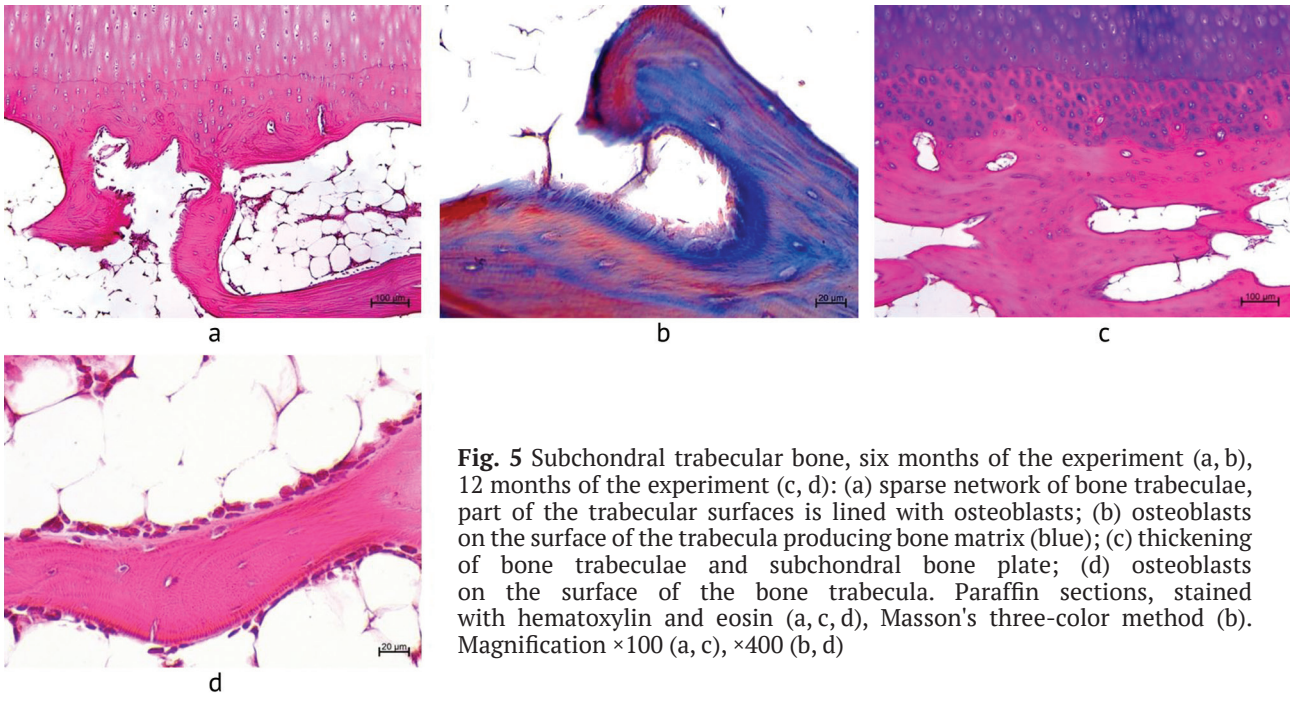

Fig. 5 Subchondral trabecular bone, six months of the experiment (a, b), 12 months of the experiment (c, d): (a) sparse network of bone trabeculae, part of the trabecular surfaces is lined with osteoblasts; (b) osteoblasts on the surface of the trabecula producing bone matrix (blue); (c) thickening of bone trabeculae and subchondral bone plate; (d) osteoblasts on the surface of the bone trabecula. Paraffin sections, stained with hematoxylin and eosin (a, c, d), Masson's three-color method (b). Magnification ×100 (a, c), ×400 (b, d)

Histomorphometric analysis after six months of the experiment did not reveal any significant differences in the values of the thickness parameters of non-calcified and calcified cartilage relative to the control group; a statistically significant decrease in the thickness of the subchondral bone plate was noted, and differences in the values of the bone index in the subchondral trabecular bone were at the level of a statistical tendency (Table 1).

After 12 months of the experiment, a statistically significant decrease in non-calcified cartilage thickness and an increase in calcified cartilage thickness, indicating a statistical tendency, were recorded when compared with the control group. In the subchondral zone, the median subchondral bone plate thickness was 33 % greater than in the control group, and the median bone index

in the subchondral trabecular bone was 31 % greater. Differences from the control group were a statistical tendency while the differences between the experimental time points were statistically significant (Table 1).

Table 1

Histomorphometric characteristics of articular cartilage and subchondral zone of the tibia at the experimental time points and in control rabbits (Me (Q1; Q3) [min–max])

Parameters	Findings		
	Control group	6 months	12 months
Thickness (height) of uncalcified cartilage ($h_{uncal.cr}$, μm)	1.28 (1.21; 1.33) [1.16–1.66]	1.24 (1.18; 1.32) [1.15–1.79] p = 0.5823	1.15 (1.09; 1.18) [1.01–1.24] **p = 0.0013; p^1 = 0.0045**
Thickness of calcified cartilage ($h_{cal.cr}$, μm)	125.93 (104.68; 135.66) [95.98–173.84]	120.34 (105.43; 129.24) [75.36–189.76] p = 0.9081	154.46 (132.39; 155.83) [89.14–190.83] p = 0.0576; p^1 = 0.1552
Subchondral bone plate thickness (h_{CtTh}, μm)	144.11 (87.55; 205.31) [60.92–223.87]	97.44 (87.97; 172.96) [60.92–167.86] **p = 0.0105**	195.21 (125.77; 216.51) [69.52–284.78] p = 0.1293; **p^1 = 0.0068**
Trabecula thickness (TbTh, μm)	156.47 (81.95; 234.91) [28.23–281.94]	112.91 (70.35; 140.54) [56.82–195.12] p = 0.2801	189.69 (163.06; 195.93) [64.36–436.09] p = 0.0556; **p^1 = 0.0113**
Intertrabecular space width (ItTh, μm)	267.09 (175.78; 311.26) [105.65–729.22]	312.69 (176.28; 402.02) [54.13–718.13] p = 0.9181	216.58 (160.04; 230.24) [62.92–429.26] p = 0.0552; p^1 = 0.0598
TbTh / ItTh	0.69 (0.31; 0.75) [0.26–2.66]	0.56 (0.25; 0.73) [0.14–1.97] p = 0.3284	0.91 (0.48; 0.82) [0.27–2.82] p = 0.0571; **p^1 = 0.0261**

Note: p — level of significance of differences when compared with the control, p^1 — level of significance of differences between the time points of the experiment according to the Mann – Whitney criterion, $p \leqslant 0{,}05$. Statistically significant differences are highlighted in bold, differences at the level of statistical tendency are in italics.

Morphological assessment of the synovial membrane according to the scale of Krenn et al. [26] indicated mild synovitis in all animals after six months of the experiment and in 30 % of cases after 12 months of the experiment (in 70 % of cases, synovitis was not detected). Structural changes in the articular cartilage according to the OARSI scale [16] after six months of the experiment corresponded to grade 1 in most cases (30 % — grade 0), after 12 months in 70 % of cases it was grade 1, and in 30 % grade 2. Structural changes in the subchondral zone according to the scale of Aho et al. [17] after six months of the experiment corresponded to grade 0 of "very early changes", when subchondral sclerosis is absent, and the subchondral bone plate is thinned. After 12 months of the experiment, an increase in the median thickness of the subchondral bone plate and an increase in the volume of trabecular bone indicated focal subchondral sclerosis and corresponded to grade 1 (Table 2).

Table 2

Analysis of the results of the assessment of structural changes in joint components at the stages of the experiment

N	Experiment stage	Results		
		Krenn et al., points	OARSI, grade	Aho et al., grade
1	6 months	2	0	0
2	6 months	2	1	0
3	6 months	3	1	0
4	12 months	2	2	1
5	12 months	1	1	1
6	12 months	1	1	1

DISCUSSION

The study conducted provided a comprehensive assessment of the structural reorganization of the main components of the joint after application of a calcium-phosphate coated implant to the adjacent limb segment in the late stages of prosthesis fitting.

According to current concepts, the initial changes in osteoarthritis, arising from macro- or microdamage, occur at the molecular level and activate pathological adaptive restorative responses, including pro-inflammatory pathways of the immune system [27]. It is known that the synovial environment in osteoarthritis is characterized by hyperplasia of the synovial membrane, the formation of synovial pannus, an increase in the representation of macrophage-like synoviocytes, and increased infiltration of immune cells. M1-polarized macrophages and activated fibroblast-like synoviocytes and fibroblasts produce pro-inflammatory cytokines, which, in turn, are responsible for increased synthesis and expression of matrix metalloproteinases that destroy articular cartilage [28, 29]. Simultaneously with changes in the cartilage, structural changes are recorded in the underlying subchondral zone, sclerosis of the subchondral bone, extensive remodeling of trabeculae, the formation of foci of necrosis and osteophytes in the marginal areas of the joint [30].

This study demonstrated that mild synovitis was detected in the adjacent joint in most cases at six months after prosthesis application. This synovitis was characterized by hyperplasia of the integumentary layer, an increased proportion of macrophage-like synovial cells, and the presence of plasma and mast cells in the subsynovial layer. Histological signs of impaired synovial blood supply (narrowing of the microvascular lumen) were recorded throughout the experiment. Mild synovitis, detected at six months, was reversible in most cases after 12 months (it persisted in one case and was accompanied by synovial pannus invasion into the superficial zone of the articular cartilage).

Histological signs of inflammation of the synovial membrane under these experimental conditions are characteristic of non-infectious synovitis [26] and may be caused by damage to nerve fibers and/or disruption of joint biomechanics.

The study of the biomechanical factors of knee osteoarthritis by Esposito et al. showed that patients with transtibial amputation have an increased risk of developing this disease [31].

Inflammation and impaired blood supply to the synovial membrane have a negative impact on the structure of articular cartilage through several mechanisms, including the release of inflammatory mediators, impaired transport of nutrients and the removal of metabolic products through diffusion [32].

Throughout the experiment, ingrowth of vessel from the subchondral zone into the deep zone of non-calcified cartilage was observed. The penetration of blood vessels into cartilage is a pathological process that can lead to its destruction and replacement with fibrous and/or bone tissue. Anti-angiogenic factors produced by chondrocytes help prevent this process. It was established that the severity of articular cartilage damage correlates with the number of newly formed blood vessels [33, 34].

Histomorphometrically, a statistically significant decrease in non-calcified cartilage thickness values relative to the control group was recorded by the end of the experiment, while calcified cartilage thickness values were significantly greater. In the subchondral zone, morphometric parameters varied widely both in the control group and throughout the experiment. By the end of the experiment, the median values for the subchondral bone plate thickness and subchondral trabecular bone index parameters were greater than those in the control group. The observed difference in subchondral bone plate thickness and subchondral zone bone index compared to the control group is not statistically significant, but tends to be significant ($p < 0.1$), requiring further studies with a larger sample size to confirm or refute this tendency.

Staining with the three-color method according to Masson detected that fuchsinophilic structures predominated in the subchondral bone plate and subchondral trabecular bone; the surfaces of the bone trabeculae were lined with active osteoblasts, which indirectly indicated the positive effect of the calcium phosphate coating of the implant on the processes of reparative osteogenesis and mineralization of the bone matrix.

Subchondral sclerosis in osteoarthritis is the result of compensatory and adaptive reactions in response to decreased mineralization of the bone matrix, aimed at maintaining the structure of hyaline cartilage under mechanical load and preventing its further destruction [35, 36]. The key factor in osteoarthritis is not subchondral sclerosis itself, but increased bone tissue remodeling and decreased mineralization of the bone matrix [35, 37]. The histological signs of inflammation and impaired blood supply to the synovial membrane, invasion of the synovial pannus into the superficial zone of cartilage, thinning of the articular cartilage, and penetration of blood vessels into the deep zone of non-calcified cartilage from the subchondral zone identified in this study are prognostic histological markers of osteoarthritis.

The obtained knowledge about the structural reorganization of the main components of the joint adjacent to the prosthesis in the late stages after prosthetic application is of great importance for the development of an optimal therapeutic strategy aimed at slowing the progression of osteoarthritis.

CONCLUSION

Structural changes in the osteochondral component of the tibial plateau one year after application of a tibial calcium phosphate-coated implant were consistent with the initial stage of osteoarthritis. Mild non-infectious synovitis was reversible. The use of calcium phosphate-coated implants promoted the activation of reparative osteogenesis and mineralization of the bone matrix in the subchondral zone.

Conflict of interests *Not declared*

Source of funding *The work was supported by the program of the Ministry of Health of the Russian Federation within the framework of the state assignment at the Federal State Budgetary Institution National Ilizarov Medical Research Center of Traumatology and Orthopedics for the implementation of the research in 2024–2026.*

The authors bear full responsibility for submitting the final version of the manuscript for publication.

All authors participated in the development of the study's concept and writing the manuscript. The final version of the manuscript was approved by all authors.

REFERENCES

1. Li Y, Felländer-Tsai L. The bone anchored prostheses for amputees - Historical development, current status, and future aspects. *Biomaterials*. 2021;273:120836. doi: 10.1016/j.biomaterials.2021.120836.
2. Hoellwarth JS, Tetsworth K, Rozbruch SR, et al. Osseointegration for Amputees: Current Implants, Techniques, and Future Directions. *JBJS Rev*. 2020;8(3):e0043. doi: 10.2106/JBJS.RVW.19.00043.
3. Wnuk-Scardaccione A, Bilski J. Breaking Barriers-The Promise and Challenges of Limb Osseointegration Surgery. *Medicina (Kaunas)*. 2025;61(3):542. doi: 10.3390/medicina61030542.
4. Stock L, Seyboldt LF, Wilkens P, Braatz F. Osseointegration in amputation surgery : Representative studies. *Unfallchirurgie (Heidelb)*. 2025;128(4):248-255. (In German) doi: 10.1007/s00113-025-01542-5.
5. Sinegub AV, Kovalenko DA, Chupryaev VA, et al. Complications of Osseointegrated prostheses and comparison of quality of life in patients with different prosthetic systems: A review. *Traumatology and Orthopedics of Russia*. 2025;31(2):178-189. (In Russ.) doi: 10.17816/2311-2905-17663.
6. Örgel M, Schwarze F, Graulich T, et al. Comparison of functional outcome and patient satisfaction between patients with socket prosthesis and patients treated with transcutaneous osseointegrated prosthetic systems (TOPS) after transfemoral amputation. *Eur J Trauma Emerg Surg*. 2022;48(6):4867-4876. doi: 10.1007/s00068-022-02018-6.
7. Tropf JG, Potter BK. Osseointegraton for amputees: Current state of direct skeletal attachment of prostheses. *Orthoplast Surg*. 2023;12:20-28. doi: 10.1016/j.orthop.2023.05.004.
8. Tereshenko V, Giorgino R, Eberlin KR, et al. Emerging Value of Osseointegration for Intuitive Prosthetic Control after Transhumeral Amputations: A Systematic Review. *Plast Reconstr Surg Glob Open*. 2024;12(5):e5850. doi: 10.1097/GOX.0000000000005850.
9. Mortazavi SMJ, Abbaspour A, Seyedtabaei SMM, et al. Improving quality of life for transfemoral amputees: results from a two-year study of the OPRA implant system and rehabilitation protocol. *Eur J Orthop Surg Traumatol*. 2025;35(1):85. doi: 10.1007/s00590-025-04221-8.
10. Hou C, An J, Zhao D, et al. Surface Modification Techniques to Produce Micro/Nano-scale Topographies on Ti-Based Implant Surfaces for Improved Osseointegration. *Front Bioeng Biotechnol*. 2022;10:835008. doi: 10.3389/fbioe.2022.835008.

11. Pettersen E, Anderson J, Ortiz-Catalan M. Electrical stimulation to promote osseointegration of bone anchoring implants: a topical review. *J Neuroeng Rehabil*. 2022;19(1):31. doi: 10.1186/s12984-022-01005-7.
12. Łosiewicz B, Osak P, Nowińska D, Maszybrocka J. Developments in dental implant surface modification. *Coatings*. 2025;15(1):109. doi: 10.3390/coatings15010109.
13. Ziegelmeyer T, Martins de Sousa K, Liao TY, et al. Multifunctional micro/nano-textured titanium with bactericidal, osteogenic, angiogenic and anti-inflammatory properties: Insights from *in vitro* and *in vivo* studies. *Mater Today Bio*. 2025;32:101710. doi: 10.1016/j.mtbio.2025.101710.
14. Korytkin AA, Orlinskaya NY, Novikova YS, et al. Biocompatibility and Osseointegration of Calcium Phosphate-Coated and Non-Coated Titanium Implants with Various Porosities. *Sovrem Tekhnologii Med*. 2021;13(2):52-57. doi: 10.17691/stm2021.13.2.06.
15. Stogov MV, Emanov AA, Kuznetsov VP, et al. The effect of zinc-containing calcium phosphate coating on the osseointegration of transcutaneous implants for limb prosthetics. *Genij Ortopedii*. 2024;30(5):677-686. doi: 10.18019/1028-4427-2024-30-5-677-686.
16. Pritzker KP, Gay S, Jimenez SA, et al. Osteoarthritis cartilage histopathology: grading and staging. *Osteoarthritis Cartilage*. 2006;14(1):13-29. doi: 10.1016/j.joca.2005.07.014.
17. Aho O-M, Finnila M, Thevenot J, et al. Subchondral bone histology and grading in osteoarthritis. *PLoS One*. 2017;12(3):e0173726. doi: 10.1371/journal.pone.0173726.
18. Stupina TA, Emanov AA, Kuznetsov VP, Ovchinnikov EN. Assessment of knee osteoarthritis risk following canine tibial prosthetics (pilot experimental morphological study). *Genij Ortopedii*. 2021;27(6):795-799. doi: 10.18019/1028-4427-2021-27-6-795-799.
19. Stupina TA, Emanov AA, Kuznetsov VP, Ovchinnikov EN. Remodeling of articular cartilage and subchondral zone of the tibia in exo-prosthetics of the limb. *Genij Ortopedii*. 2025;31(3):341-349. doi: 10.18019/1028-4427-2025-31-3-341-349.
20. Bowker HK, Michael JW. *Atlas of Limb Prosthetics: Surgical, Prosthetic, and Rehabilitation Principles*. St. Louis: Mosby Year Book; 1992:930
21. Susliaev VG, Shcherbina KK, Smirnova LM, et al. Early prosthetic and orthopedic assistance in medical rehabilitation of children with congenital and amputation defects of the lower limbs. *Genij Ortopedii*. 2020;26(2):198-205. doi: 10.18019/1028-4427-2020-26-2-198-205.
22. Mathiessen A, Conaghan PG. Synovitis in osteoarthritis: current understanding with therapeutic implications. *Arthritis Res Ther*. 2017;19(1):18. doi: 10.1186/s13075-017-1229-9.
23. Kuznetsov VP, Gorgots VG, Anikeev AV, et al. *Tubular bone stump implant*. Patent RF, no.194912, 2019. Available at: https://www.fips.ru/registers-doc-view/fips_servlet?DB=RUPM&DocNumber=194912&TypeFile=html. Accessed Jan 16, 2026. (In Russ.)
24. Kuznetsov VP, Gubin AV, Gorgots VG, et al. *Device for osseointegration of the implant into the bone of the stump of the lower limb*. Patent RF, № 185647, 2018. Available at: https://www.fips.ru/registers-doc-view/fips_servlet?DB=RUPM&DocNumber=185647&TypeFile=html. Accessed Jan 16, 2026. (In Russ.)
25. Zhang C, Yan B, Cui Z, et al. Bone regeneration in minipigs by intrafibrillarly-mineralized collagen loaded with autologous periodontal ligament stem cells. *Sci Rep*. 2017;7(1):10519. doi: 10.1038/s41598-017-11155-7
26. Krenn V, Morawietz L, Burmester GR, et al. Synovitis score: discrimination between chronic low-grade and high-grade synovitis. *Histopathology*. 2006;49(4):358-364. doi: 10.1111/j.1365-2559.2006.02508.x.
27. Alekseeva LI, Taskina EA, Kashevarova NG. Osteoarthritis: epidemiology, classification, risk factors, and progression, clinical presentation, diagnosis, and treatment. *Modern Rheumatology Journal*. 2019;13(2):9-21. (In Russ.) doi: 10.14412/1996-7012-2019-2-9-21.
28. Raymuev KV, Ishenko AM, Malyshev ME. Pro-inflammatory and anti-inflammatory cytokines in the pathogenesis of osteoarthritis. *Herald of North-Western State Medical University named after I.I. Mechnikov*. 2018;10(3):19-27. (In Russ.) doi: 10.17816/mechnikov201810319-27.
29. Dydykina IS, Arutyunova EV, Kovalenko PS, et al. Synovitis in osteoarthritis: the current state of the problem. *Modern Rheumatology Journal*. 2021;15(2):120-125. (In Russ.) doi: 10.14412/1996-7012-2021-2-120-125.
30. Donell S. Subchondral bone remodelling in osteoarthritis. *EFORT Open Rev*. 2019;4(6):221-229. doi: 10.1302/2058-5241.4.180102.
31. Russell Esposito E, Wilken JM. Biomechanical risk factors for knee osteoarthritis when using passive and powered ankle-foot prostheses. *Clin Biomech (Bristol)*. 2014;29(10):1186-1192. doi: 10.1016/j.clinbiomech.2014.09.005.
32. van der Kraan PM. The Interaction between Joint Inflammation and Cartilage Repair. *Tissue Eng Regen Med*. 2019;16(4):327-334. doi: 10.1007/s13770-019-00204-z.
33. Fransès RE, McWilliams DF, Mapp PI, Walsh DA. Osteochondral angiogenesis and increased protease inhibitor expression in OA. *Osteoarthritis Cartilage*. 2010;18(4):563-571. doi: 10.1016/j.joca.2009.11.015.
34. Zhao Z, Sun X, Tu P, et al. Mechanisms of vascular invasion after cartilage injury and potential engineering cartilage treatment strategies. *FASEB J*. 2024;38(6):e23559. doi: 10.1096/fj.202302391RR.
35. Cox LG, van Donkelaar CC, van Rietbergen B, et al. Decreased bone tissue mineralization can partly explain subchondral sclerosis observed in osteoarthritis. *Bone*. 2012;50(5):1152-1161. doi: 10.1016/j.bone.2012.01.024.
36. Stewart HL, Kawcak CE. The Importance of Subchondral Bone in the Pathophysiology of Osteoarthritis. *Front Vet Sci*. 2018;5:178. doi: 10.3389/fvets.2018.00178.
37. Goetzen M, Hofmann-Fliri L, Arens D. et al. Subchondral screw abutment: does it harm the joint cartilage? An *in vivo* study on sheep tibiae. *Int Orthop*. 2017;41(8):1607-1615. doi: 10.1007/s00264-017-3404-7.

The article was submitted 17.12.2025; approved after reviewing 23.12.202; accepted for publication 09.02.2026.

Information about the authors:

Tatyana A. Stupina — Doctor of Biological Sciences, Leading Researcher, StupinaSTA@mail.ru, https://orcid.org/0000-0003-3434-0372;

Andrey A. Emanov — Candidate of Veterinary Sciences, Leading Researcher, a_eman@list.ru, https://orcid.org/0000-0003-2890-3597;

Viktor P. Kuznetsov — Doctor of Technical Sciences, Professor, Head of Laboratory, wpkuzn@mail.ru, https://orcid.org/0000-0001-8949-6345.